

A low-order preconditioner for high-order element-wise divergence constant finite element spaces

Jeferson W. D. Fernandes¹, Nathan Shauer¹, Philippe R. B. Devloo¹

¹LabMeC-FECAU-Universidade Estadual de Campinas
R. Josiah Willard Gibbs 85, 13083-841, Campinas-SP, Brazil
jwdf@unicamp.br; nathan.sh@gmail.com, phil@unicamp.br

Abstract. Mixed finite element problems are a class of problems that arises when modeling several physical phenomena, such as in computational fluid dynamics, structural analysis, optimization, etc. Designing efficient iterative schemes for such a family of approximations has been the subject of several works in the past decades. However, its success is intimately related to the proper definition of a preconditioner, i. e., the projection of the original algebraic system to an equivalent one with better spectral properties. In recent work, we have proposed a new class of $H(\text{div})$ -conforming finite element spaces with element-wise constant divergent. This family of elements was designed to improve reservoir simulation computational cost and are obtained by choosing the lower order space with piece-wise constant normal fluxes incremented with divergence-free higher-order functions. In this work, we propose an iterative scheme to solve problems arising in the context of the above mentioned element-wise constant divergence approximation spaces. The strategy consists on using the matrix of linear fluxes as a preconditioner to solve the higher-order flux problem. The latter is solved iteratively by means of a conjugate gradient scheme. In the presented numerical tests, this strategy has shown to be convergent in a few iterations for different problems in 2D and 3D. In addition, as internal fluxes are condensed, only boundary variables need to be computed. This strategy relates to the MHM technique and can be efficiently used to access fast multi-scale approximations in future work.

Keywords: Preconditioning, Iterative methods, Finite Element Method, Mixed approximations.

1 Introduction

Mixed finite element are a class of problems which arises when modeling several physical phenomena, such as in computational fluid dynamics, structural analysis, optimization etc. It is named as *mixed* because more than one field is approximated, and usually one of them plays the role of Lagrange multipliers. As it consists in a *saddle point problem*, direct solvers (usually based on Gaussian elimination or LU/Cholesky decomposition) may suffer with low convergence due to the frequent presence of null pivots. In addition, iterative methods are preferred when solving both large and sparse problems, as they present much lower computational cost, when properly preconditioned [1].

The main issue, when using iterative methods, is to ensure its convergence in an acceptable number of iterations, which may be related to the spectral properties of the corresponding matrix. The solution of saddle point problems may be subdivided into two categories[1]: segregated and coupled methods. In the first, the fields being approximated are computed separately and most of them are variations of the Uzawa's method [2] while in the latter an approximation for both field is obtained simultaneously (see for instance [1, 3, 4] for a complete review on the subject).

Using low-order preconditioners to approximate high-order discretizations is a well known technique, which has been successfully applied specially to spectral discretizations. Its first use dates the 80's with the work of Orszag [5], where finite difference techniques were applied as preconditioners to spectral discretizations. Still in the context of spectral methods, this idea has been further developed to several different applications such as the incompressible Navier-Stokes equations[6] (see for instance [7] and references therein).

More recently, [8], presented low-order preconditioning technique based on nodal high order triangular finite elements, with nodes not necessarily coincident in both scales, but connected by means of a least-squares operator.

A technique for preconditioning high-order Lagrangian finite elements bases on an auxiliary linear element stiffness matrix is also presented by [9], where the authors obtain a preconditioner with condition number inde-

pendent of the mesh size.

This idea has also been explored in other physical problems such as elasticity [10], the Maxwell's equations [11]. Particularly, in the last example, Pazner et al. [11] developed several low-order preconditioners exploring the de Rham complex properties, based on the spectral equivalence of low-order discretizations for higher-order $H(\text{div})$ and $H(\text{curl})$ spaces demonstrated by [12].

In this work, we extend this principle also for conforming $H(\text{div})$ finite element discretizations. More specifically, we develop an iterative scheme over a particular $H(\text{div})$ -FE space, with element-wise constant divergent. This FE space is suitable for simulations involving element-wise constant pressures or source terms, with a lower computational cost and has been introduced by the authors in [13]. Roughly speaking, the method consists in uncoupling constant and higher-order normal fluxes and use the former as a preconditioner for solving the latter.

The paper is organized as follows: in Section 2, a model problem is presented; in Section 3 the model problem is solved by means of the element-wise divergence constant finite element space; both 2D and 3D numerical results are presented in Section 4 and concluding remarks are drawn in Section 5.

2 Model problem

Firstly, we consider an open domain Ω with a Lipschitz boundary $\Gamma = \Gamma_D \cup \Gamma_N$, where Γ_D and a Γ_N refers to partitions corresponding to Dirichlet and Neumann conditions, respectively. The model problem considered throughout this work is the mixed version of the Poisson's equation, which reads: find the flux $\boldsymbol{\sigma} \in H(\text{div}, \Omega)$ and pressure $u \in L^2(\Omega)$ fields such that

$$\begin{aligned} \boldsymbol{\sigma} &= -\mathbb{K}\nabla u && \text{in } \Omega, \\ \nabla \cdot \boldsymbol{\sigma} &= f && \text{in } \Omega, \\ u &= u_D && \text{on } \Gamma_D, \\ \boldsymbol{\sigma} \cdot \mathbf{n} &= g && \text{on } \Gamma_N, \end{aligned} \tag{1}$$

where \mathbb{K} is the permeability tensor, $u_D \in H^{1/2}(\Gamma_D)$, $g \in L^2(\Gamma_N)$ and $f \in L^2(\Omega)$ are given functions and \mathbf{n} is the outward unit vector.

2.1 Weak statement

The standard construction of a weak statement for problem (1) *via* Galerkin's method is defined as: find $\boldsymbol{\sigma} \in H(\text{div}, \Omega)$, with $\boldsymbol{\sigma} \cdot \mathbf{n}|_{\Gamma_D} = g$, and $u \in L^2(\Omega)$ such that

$$\begin{aligned} \int_{\Omega} \mathbb{K}^{-1} \boldsymbol{\sigma} \cdot \mathbf{w}_{\boldsymbol{\sigma}} \, d\mathbf{x} - \int_{\Omega} u \nabla \cdot \mathbf{w}_{\boldsymbol{\sigma}} \, d\mathbf{x} &= - \int_{\Gamma_D} u_D \llbracket \mathbf{w}_{\boldsymbol{\sigma}} \rrbracket ds \quad \forall \mathbf{w}_{\boldsymbol{\sigma}} \in H(\text{div}, \Omega), \\ \int_{\Omega} \nabla \cdot \boldsymbol{\sigma} w_u \, d\mathbf{x} &= \int_{\Omega} f w_u \, d\mathbf{x} \quad \forall w_u \in L^2(\Omega), \end{aligned} \tag{2}$$

and the discretization of (2) can be performed by means of finite element methods [14].

For instance, to discretize (2) in terms of a FE approximation we define a single discretization parameter $\gamma = (h, k)$, where h represents the mesh characteristic size and k is related to the polynomial degree. We also consider a conformal partition $\mathcal{T}_h = K$ and introduce the following finite dimensional spaces:

$$\mathbf{V}^{\gamma} = \{ \boldsymbol{\sigma} \in H(\text{div}, \Omega) : \boldsymbol{\sigma}|_K \in \mathbf{V}_k, K \in \mathcal{T}_h \}, \tag{3}$$

$$W^{\gamma} = \{ u \in L^2(\Omega) : u|_K \in W_k, K \in \mathcal{T}_h \}. \tag{4}$$

Then, the finite dimensional version of problem (2) can be stated as: find $\boldsymbol{\sigma}^{\gamma} \in \mathbf{V}^{\gamma}$, with $\boldsymbol{\sigma}^{\gamma} \cdot \mathbf{n}|_{\Gamma_D} = g$, and $u^{\gamma} \in W^{\gamma}$ such that

$$\begin{aligned} \int_{\Omega} \mathbb{K}^{-1} \boldsymbol{\sigma}^{\gamma} \cdot \mathbf{w}_{\boldsymbol{\sigma}}^{\gamma} \, d\mathbf{x} - \int_{\Omega} u^{\gamma} \nabla \cdot \mathbf{w}_{\boldsymbol{\sigma}}^{\gamma} \, d\mathbf{x} &= - \int_{\Gamma_D} u_D \llbracket \mathbf{w}_{\boldsymbol{\sigma}}^{\gamma} \rrbracket ds \quad \forall \mathbf{w}_{\boldsymbol{\sigma}}^{\gamma} \in \mathbf{V}^{\gamma}, \\ \int_{\Omega} \nabla \cdot \boldsymbol{\sigma}^{\gamma} w_u^{\gamma} \, d\mathbf{x} &= \int_{\Omega} f w_u^{\gamma} \, d\mathbf{x} \quad \forall w_u^{\gamma} \in W^{\gamma}. \end{aligned} \tag{5}$$

3 Element-wise divergence constant FE spaces and the iterative scheme

In a recent work [13], we coauthored a work that introduced an element-wise divergence-constant flux approach in the context of exact finite element de Rham approximations. It consists in a filtered version of the standard $H(\text{div})$ approximations suitable for particular cases where the source term f is an element-wise constant function. It may be noticed, however, that it does not represent a limitation of the iterative method presented in the following.

More specifically, these element-wise divergence constant FE spaces are defined as

$$\mathbf{V}_c^\gamma = \{\boldsymbol{\sigma}_c^\gamma \in \mathbf{V}^\gamma : \nabla \cdot \boldsymbol{\sigma}_c^\gamma \in W_0\}, \quad (6)$$

and are built by extending constant normal flux functions over the facets $\bar{\boldsymbol{\sigma}}^\gamma \in \bar{\mathbf{V}}^\gamma$ (RT_0 Raviart-Thomas finite elements [15]) to the interior of the element. The remaining functions are composed of divergence-free internal (namely *bubble* functions) and edge higher-order functions $\mathring{\boldsymbol{\sigma}}^\gamma \in \mathring{\mathbf{V}}^\gamma$, such that

$$\bar{\mathbf{V}}^\gamma = \{\bar{\boldsymbol{\sigma}}^\gamma \in H(\text{div}, \Omega) : \nabla \cdot \bar{\boldsymbol{\sigma}}^\gamma = c, \gamma = (h, 0)\}, \quad (7)$$

$$\mathring{\mathbf{V}}^\gamma = \{\mathring{\boldsymbol{\sigma}}^\gamma \in H(\text{div}, \Omega) : \nabla \cdot \mathring{\boldsymbol{\sigma}}^\gamma = 0\}, \quad (8)$$

where c is an arbitrary constant and the following sum holds $\mathbf{V}_c^\gamma = \bar{\mathbf{V}}^\gamma \oplus \mathring{\mathbf{V}}^\gamma$.

Under such considerations, the formulation (2) employing element-wise divergence constant spaces can be rewritten and is stated as: find $\bar{\boldsymbol{\sigma}}^\gamma \in \bar{\mathbf{V}}^\gamma$, with $\bar{\boldsymbol{\sigma}}^\gamma \cdot \mathbf{n}|_{\Gamma_N} = \Pi_\gamma^N \bar{\boldsymbol{\sigma}}_N^\gamma$, $\mathring{\boldsymbol{\sigma}}^\gamma \in \mathring{\mathbf{V}}^\gamma$, with $\mathring{\boldsymbol{\sigma}}^\gamma \cdot \mathbf{n}|_{\Gamma_N} = \Pi_\gamma^N \mathring{\boldsymbol{\sigma}}_N^\gamma$, and $u_0^\gamma \in W_0^\gamma$ such that

$$\begin{aligned} \int_\Omega \mathbb{K}^{-1} \bar{\boldsymbol{\sigma}}^\gamma \cdot \mathbf{w}_\sigma^\gamma \, d\mathbf{x} + \int_\Omega \mathbb{K}^{-1} \mathring{\boldsymbol{\sigma}}^\gamma \cdot \mathbf{w}_\sigma^\gamma \, d\mathbf{x} - \int_\Omega u_0^\gamma \nabla \cdot \mathbf{w}_\sigma^\gamma \, d\mathbf{x} &= - \int_{\Gamma_D} \llbracket \mathbf{w}_\sigma^\gamma \rrbracket u_D \, ds \quad \forall \mathbf{w}_\sigma^\gamma \in \bar{\mathbf{V}}^\gamma, \\ \int_\Omega \mathbb{K}^{-1} \bar{\boldsymbol{\sigma}}^\gamma \cdot \mathbf{w}_\sigma^\gamma \, d\mathbf{x} + \int_\Omega \mathbb{K}^{-1} \mathring{\boldsymbol{\sigma}}^\gamma \cdot \mathbf{w}_\sigma^\gamma \, d\mathbf{x} &= - \int_{\Gamma_D} \llbracket \mathbf{w}_\sigma^\gamma \rrbracket u_D \, ds \quad \forall \mathbf{w}_\sigma^\gamma \in \mathring{\mathbf{V}}^\gamma, \\ \int_\Omega \nabla \cdot \bar{\boldsymbol{\sigma}}^\gamma w_u^\gamma \, d\mathbf{x} &= \int_\Omega f w_u^\gamma \, d\mathbf{x} \quad \forall w_u^\gamma \in W_0. \end{aligned} \quad (9)$$

Formulation (9) can also be represented in a hybridized form, by weakly imposing continuity of $\bar{\boldsymbol{\sigma}}^\gamma$ by a constant Lagrange multiplier. For this purpose we define the following FE space:

$$\Lambda_u^\gamma = \{\mu^\gamma \in W^\gamma(\Gamma_K)\}. \quad (10)$$

In such case, the formulation is stated as find $\bar{\boldsymbol{\sigma}}^\gamma \in \bar{\mathbf{V}}^\gamma$, with $\bar{\boldsymbol{\sigma}}^\gamma \cdot \mathbf{n}|_{\Gamma_N} = \Pi_\gamma^N \bar{\boldsymbol{\sigma}}_N^\gamma$, $\mathring{\boldsymbol{\sigma}}^\gamma \in \mathring{\mathbf{V}}^\gamma$, with $\mathring{\boldsymbol{\sigma}}^\gamma \cdot \mathbf{n}|_{\Gamma_N} = \Pi_\gamma^N \mathring{\boldsymbol{\sigma}}_N^\gamma$, $u_0^\gamma \in W_0$ and $\mu^\gamma \in \Lambda_u^\gamma$ such that

$$\begin{aligned} \int_\Omega \mathbb{K}^{-1} \bar{\boldsymbol{\sigma}}^\gamma \cdot \mathbf{w}_\sigma^\gamma \, d\mathbf{x} + \int_\Omega \mathbb{K}^{-1} \mathring{\boldsymbol{\sigma}}^\gamma \cdot \mathbf{w}_\sigma^\gamma \, d\mathbf{x} \\ - \int_\Omega u_0^\gamma \nabla \cdot \mathbf{w}_\sigma^\gamma \, d\mathbf{x} + \int_{\Gamma_e} \mu^\gamma \llbracket \mathbf{w}_\sigma^\gamma \rrbracket \, ds &= - \int_{\Gamma_D} u_D \llbracket \mathbf{w}_\sigma^\gamma \rrbracket \, ds \quad \forall \mathbf{w}_\sigma^\gamma \in \bar{\mathbf{V}}^\gamma, \\ \int_\Omega \mathbb{K}^{-1} \bar{\boldsymbol{\sigma}}^\gamma \cdot \mathbf{w}_\sigma^\gamma \, d\mathbf{x} + \int_\Omega \mathbb{K}^{-1} \mathring{\boldsymbol{\sigma}}^\gamma \cdot \mathbf{w}_\sigma^\gamma \, d\mathbf{x} &= \int_{\Gamma_D} u_D \llbracket \mathbf{w}_\sigma^\gamma \rrbracket \, ds \quad \forall \mathbf{w}_\sigma^\gamma \in \mathring{\mathbf{V}}^\gamma, \\ \int_\Omega \nabla \cdot \bar{\boldsymbol{\sigma}}^\gamma w_u^\gamma \, d\mathbf{x} &= \int_\Omega f w_u^\gamma \, d\mathbf{x} \quad \forall w_u^\gamma \in W_0^\gamma, \\ \int_{\Gamma_e} w_\mu^\gamma \llbracket \bar{\boldsymbol{\sigma}}^\gamma \rrbracket \, ds &= 0 \quad \forall w_\mu^\gamma \in \Lambda_u^\gamma. \end{aligned} \quad (11)$$

Problem (11) can also be represented in a matrix form as

$$\begin{bmatrix} \mathbf{K}_{\bar{\boldsymbol{\sigma}}\bar{\boldsymbol{\sigma}}} & \mathbf{K}_{\bar{\boldsymbol{\sigma}}\mathring{\boldsymbol{\sigma}}} & \mathbf{B}_{\bar{\boldsymbol{\sigma}}} & \mathbf{L}_{\bar{\boldsymbol{\sigma}}} \\ \mathbf{K}_{\mathring{\boldsymbol{\sigma}}\bar{\boldsymbol{\sigma}}} & \mathbf{K}_{\mathring{\boldsymbol{\sigma}}\mathring{\boldsymbol{\sigma}}} & \mathbf{0} & \mathbf{0} \\ \mathbf{B}_{\bar{\boldsymbol{\sigma}}}^T & \mathbf{0} & \mathbf{0} & \mathbf{0} \\ \mathbf{L}_{\bar{\boldsymbol{\sigma}}}^T & \mathbf{0} & \mathbf{0} & \mathbf{0} \end{bmatrix} \begin{bmatrix} \bar{\boldsymbol{\Sigma}} \\ \mathring{\boldsymbol{\Sigma}} \\ \mathbf{U}_0 \\ \mathbf{M} \end{bmatrix} = \begin{bmatrix} \mathbf{f}_{\bar{\boldsymbol{\sigma}}} \\ \mathbf{f}_{\mathring{\boldsymbol{\sigma}}} \\ \mathbf{f}_{u_0} \\ \mathbf{0} \end{bmatrix}. \quad (12)$$

Static condensation [16] can be applied to problem (12) where both $\bar{\Sigma}$ and U_0 condensed onto the Lagrange multipliers M , resulting in a matrix problem of the form

$$\begin{bmatrix} \hat{K}_{\mu\mu} & \hat{K}_{\mu\sigma} \\ \hat{K}_{\sigma\mu} & \hat{K}_{\sigma\sigma} \end{bmatrix} \begin{Bmatrix} M \\ \bar{\Sigma} \end{Bmatrix} = \begin{Bmatrix} \hat{f}_\mu \\ \hat{f}_\sigma \end{Bmatrix}. \quad (13)$$

Some properties of problem (13) needs to be highlighted. First, \bar{V}^γ is constructed in a hierarchical framework and is formed by edge and internal (bubble) functions only. In our computations, the bubble functions are also condensed onto M , which means that the only variables of $\bar{\Sigma}$ consist of higher-order edge fluxes. Another important feature is that the matrix $\hat{K}_{\mu\mu}$ corresponding to the coupling of the constant pressure Lagrange multipliers is negative definite.

The iterative strategy we propose in this work consists on solving (13) in a two-step algorithm. To properly define it, we first rewrite problem (13) as

$$\hat{K}_{\mu\mu} M = \hat{f}_\mu - \hat{K}_{\mu\sigma} \bar{\Sigma} \quad (14)$$

$$\left(\hat{K}_{\sigma\sigma} - \hat{K}_{\sigma\mu} \hat{K}_{\mu\mu}^{-1} \hat{K}_{\mu\sigma} \right) \bar{\Sigma} = \hat{f}_\sigma - \hat{K}_{\sigma\mu} \hat{K}_{\mu\mu}^{-1} \hat{f}_\mu \quad (15)$$

Then, the algorithm consists of applying the conjugate gradient method to problem (15) and a block diagonal preconditioner where the diagonal blocks are extracted from $\hat{K}_{\sigma\sigma}$. Notice that this step requires the decomposition of matrix $\hat{K}_{\mu\mu}$ which has dimension independent of the polynomial degree, as the internal fluxes and pressure are condensed and do not contribute to the size of the global system. Finally, once the system of the higher-order normal fluxes $\bar{\Sigma}$ is converged, M can be computed explicitly from (14) and, consequently, the primitive variables U_0 and $\bar{\Sigma}$ can be recovered.

4 Numerical Results

In this section we present a collection of numerical tests to evaluate the iterative scheme previously presented. In all cases a tolerance of $\varepsilon = 10^{-10}$ (Euclidean norm) was taken in the iterative process and the permeability tensor is equal to the identity, namely $\mathbb{K} = \mathbf{I}$. The formulation is evaluated for both 2D and 3D cases. In the 2D example, two cases are tested: in the first, a harmonic analytic function is taken while in the second the analysis is carried with a zero function on most parts of the computational domain, but with a peak pressure close to the center. For the 3D case, a polynomial function was used. In all cases both iteration numbers and DoF's are reported.

Another important feature concerns the boundary conditions enforcement. In all cases Dirichlet BC were considered for all boundaries. However, to suppress this variability in the analysis (type of BC), all BC DoF's were condensed.

Finally, in the 2D examples, quadrilateral finite elements are employed while hexahedral meshes are adopted in the 3D case.

4.1 2D example

Two 2D cases were considered. In the first, a harmonic analytic solution for the pressure field is taken, while in the second a rough function with a peak is chosen. Both expressions are given by (notice that the superscripts 1 and 2 denotes the first and second cases, respectively):

$$\begin{aligned} u^1 &= \sin(\pi x) \sin(\pi y), \\ u^2 &= (2^{2-(-2\pi+15x)^2-(-2\pi+15y)^2}) (5^{-(2\pi+15x)^2-(2\pi+15y)^2}) (-2\pi + 15x). \end{aligned} \quad (16)$$

Expressions for the flux field and source term can be easily derived from (16) and are omitted here.

The problem is solved in the computational domain $\Omega = [0, 1] \times [0, 1]$. The meshes employed in the analyses ranges from $n_x = n_y = 2$ up to 200. In all cases a uniform discretization was adopted, i.e., the same number of elements is taken for both x and y directions.

As previously mentioned, static condensation is applied to reduce the number of global degrees of freedom. In Table 1, we present the original global system size compared to the condensed one. Notice that the condensed problem has dimension independent on the polynomial degree. In Fig. 1 we present the plots with the number of CG iterations needed to reach convergence for polynomial degrees $k = 1$ up to 5.

Table 1. 2D example: number of equations before and after static condensation of the decomposed matrix.

n_x	#Equations					Condensed
	$k = 1$	$k = 2$	$k = 3$	$k = 4$	$k = 5$	
2	28	48	76	112	156	4
5	130	225	370	565	810	40
10	460	800	1,340	2,080	3,020	180
15	990	1,725	2,910	4,545	6,630	420
20	1,720	3,000	5,080	7,960	11,640	760
25	2,650	4,625	7,850	12,325	18,050	1,200
30	3,780	6,600	11,220	17,640	25,860	1,740
35	5,110	8,925	15,190	23,905	35,070	2,380
40	6,640	11,600	19,760	31,120	45,680	3,120
45	8,370	14,625	24,930	39,285	57,690	3,960
50	10,300	18,000	30,700	48,400	71,100	4,900
60	14,760	25,800	44,040	69,480	102,120	7,080
70	20,020	35,000	59,780	94,360	138,740	9,660
80	26,080	45,600	77,920	123,040	180,960	12,640
90	32,940	57,600	98,460	155,520	228,780	16,020
100	40,600	71,000	121,400	191,800	282,200	19,800
120	58,320	102,000	174,480	275,760	405,840	28,560
140	79,240	138,600	237,160	374,920	551,880	38,920
160	103,360	180,800	309,440	489,280	720,320	50,880
180	130,680	228,600	391,320	618,840	911,160	64,440
200	161,200	282,000	482,800	763,600	1,124,400	79,600

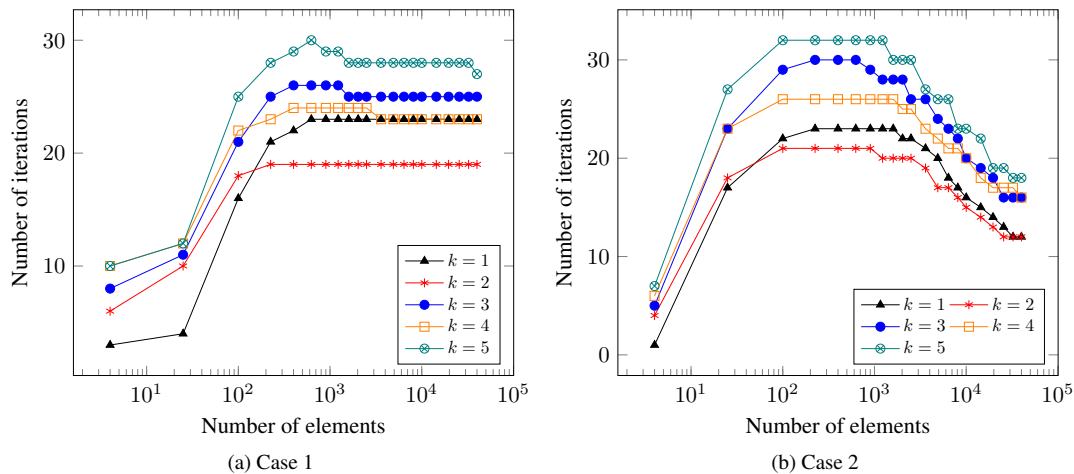


Figure 1. 2D harmonic function: number CG iterations for each iterative method.

As may be noticed, the proposed iterative scheme seems to be affected by the polynomial degree. For case 1, the number of iterations needed to convergence reaches a certain level and do not change with mesh refinement. However, when compared to case 2, the number of CG iterations increases with mesh refinement, reaches a maximum value and then decreases to a constant level, slightly lower than in the previous case. It may be related to the fact that the solution for both pressure and flux approaches zero in most of the computational domain in case 2, which coincides with the initial guess in the iterative scheme.

4.2 3D case

In this case the iterative scheme is evaluated for a 3D case whose analytic solution for the pressure field is given by:

$$u = (x - 1) x (y - 1) y (z - 1) z \tag{17}$$

The computational domain is taken as the unit cube $\Omega = [0, 1] \times [0, 1] \times [0, 1]$ and uniform hexahedral finite element meshes with $n_x = n_y = n_z$ ranging from 2 to 16 are considered for its discretization. Once again uniform discretization with the same element length in all directions was adopted.

As in the 2D cases, we present in Table 2 the reduction in the number of equations achieved with the static condensation technique. In addition, the number of CG iterations needed to reach convergence is presented for $k = 1$ up to 5 in Fig. 2.

Table 2. 3D case: number of equations before and after static condensation of the decomposed matrix.

n_x	#Equations					Condensed
	$k = 1$	$k = 2$	$k = 3$	$k = 4$	$k = 5$	
2	156	460	1,052	2,028	3,484	12
3	432	1,323	3,132	6,183	10,800	54
4	912	2,864	6,928	13,872	24,464	144
5	1,650	5,275	12,950	26,175	46,450	300
6	2,700	8,748	21,708	44,172	78,732	540
7	4,116	13,475	33,712	68,943	123,284	882
8	5,952	19,648	49,472	101,568	182,080	1,344
9	8,262	27,459	69,498	143,127	257,094	1,944
10	11,100	37,100	94,300	194,700	350,300	2,700
11	14,520	48,763	124,388	257,367	463,672	3,630
12	18,576	62,640	160,272	332,208	599,184	4,752
13	23,322	78,923	202,462	420,303	758,810	6,084
14	28,812	97,804	251,468	522,732	944,524	7,644
15	35,100	119,475	307,800	640,575	1,158,300	9,450
16	42,240	144,128	371,968	774,912	1,402,112	11,520

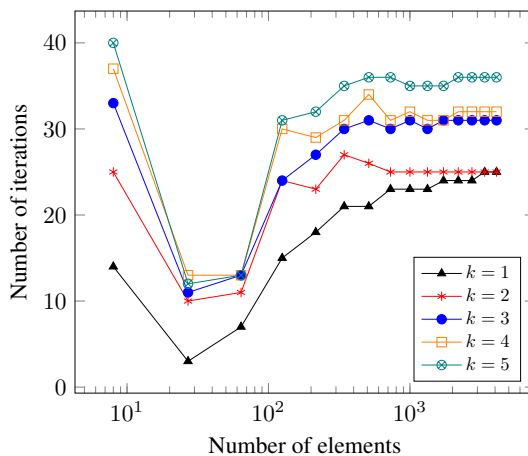


Figure 2. 3D problem: number CG iterations for each iterative method.

As may be noticed, in the 3D example presented, the proposed iterative approach performed similarly to the first 2D example, with the number of iterations increasing with mesh refinement up to a certain level kept constant.

5 Conclusions

In this work we presented an iterative scheme for higher-order flux computations based on a linear-flux preconditioner. A modified $H(div)$ -conforming space, namely $H(div)$ -constant, with element-wise constant flux divergence is employed. The flux field is partitioned into constant and higher order normal components whilst the first is used as a preconditioner to approximate the latter. In this approach, the constant flux component is hybridized and a static condensation procedure is applied, generating a 2×2 block algebraic system with negative-definite and positive-definite diagonals. This strategy expressively reduced the number of DoF's in the decomposed matrix and circumvented the original saddle point structure.

The results presented in section 4 allow us to conclude that the number of CG iterations increases with polynomial degree for the a general case and do not increase with mesh refinement.

One of the key-points in the presented method is the uncouple of constant and higher-order normal fluxes. Different results can be obtained in the case where the constant flux is employed as preconditioner for the full coupled flux field and additional tests need to be performed in this direction. Another strategies involving iterative schemes are currently under development by our research group, employing for instance multi-grid approaches.

Acknowledgements. This section should be positioned immediately after the Conclusion section. Type Acknowledgements in boldface, 10 pt Times New Roman type from left margin, leaving 20 pt line spacing before and 12pt after.

Authorship statement. The authors hereby confirm that they are the sole liable persons responsible for the authorship of this work, and that all material that has been herein included as part of the present paper is either the property (and authorship) of the authors, or has the permission of the owners to be included here.

References

- [1] D. Bertaccini and F. Durastante. Iterative Methods and Preconditioning for Large and Sparse Linear Systems with Applications. Chapman & Hall/CRC Monographs and Research Notes in Mathematics. CRC Press, 2018.
- [2] K. Arrow, L. Hurwicz, and H. Uzawa. Studies in Linear and Non-linear Programming. Stanford mathematical studies in the social sciences. Stanford University Press, 1958.
- [3] J. H. Bramble, J. E. Pasciak, and A. T. Vassilev. Analysis of the inexact uzawa algorithm for saddle point problems. SIAM Journal on Numerical Analysis, vol. 34, n. 3, pp. 1072–1092, 1997.
- [4] M. Benzi, G. H. Golub, and J. Liesen. Numerical solution of saddle point problems. Acta Numerica, vol. 14, pp. 1–137, 2005.
- [5] S. A. Orszag. Spectral methods for problems in complex geometries. Journal of Computational Physics, vol. 37, n. 1, pp. 70–92, 1980.
- [6] P. F. Fischer. An overlapping schwarz method for spectral element solution of the incompressible navier–stokes equations. Journal of Computational Physics, vol. 133, n. 1, pp. 84–101, 1997.
- [7] C. Canuto, P. Gervasio, and A. Quarteroni. Finite-element preconditioning of g-ni spectral methods. SIAM Journal on Scientific Computing, vol. 31, n. 6, pp. 4422–4451, 2010.
- [8] N. Chalmers and T. Warburton. Low-order preconditioning of high-order triangular finite elements. SIAM Journal on Scientific Computing, vol. 40, n. 6, pp. A4040–A4059, 2018.
- [9] qing Y. Huang, S. Shu, and jun X. Yu. Preconditioning higher order finite element systems by algebraic multigrid method of linear elements. Journal of Computational Mathematics, vol. 24, n. 5, pp. 657–664, 2006.
- [10] Y. Xiao and S. Shu. A robust preconditioner for higher order finite element discretizations in linear elasticity. Numerical Linear Algebra with Applications, vol. 18, n. 5, pp. 827–842, 2011.
- [11] W. Pazner, T. Kolev, and C. Dohrmann. Low-order preconditioning for the high-order finite element de rham complex, 2022.
- [12] C. R. Dohrmann. Spectral equivalence of low-order discretizations for high-order $h(\text{curl})$ and $h(\text{div})$ spaces. SIAM Journal on Scientific Computing, vol. 43, n. 6, pp. A3992–A4014, 2021.
- [13] P. R. B. Devloo, J. W. D. Fernandes, S. M. Gomes, F. Orlandini, and N. Shauer. An efficient construction of divergence-free spaces in the context of exact finite element de Rham sequences. Computer Methods in Applied Mechanics and Engineering, 2022? (no prelo).
- [14] D. Boffi, F. Brezzi, and M. Fortin. Mixed Finite Element Methods and Applications, volume 44, 2013.
- [15] P. A. Raviart and J. M. Thomas. A mixed finite element method for 2-nd order elliptic problems. In I. Galigani and E. Magenes, eds, Mathematical Aspects of Finite Element Methods, pp. 292–315, Berlin, Heidelberg. Springer Berlin Heidelberg, 1977.
- [16] R. J. GUYAN. Reduction of stiffness and mass matrices. AIAA Journal, vol. 3, n. 2, pp. 380–380, 1965.